

GreedySnake: Accelerating SSD-Offloaded LLM Training with Efficient Scheduling and Optimizer Step Overlapping

Yikang Yue^{2*} Yishu Yin^{1*} Xuehai Qian^{1†}

¹Tsinghua University, ²University of Illinois at Urbana-Champaign

Abstract

SSD-offloaded training offers a practical and promising approach to making LLM training cost-effective. Building on gradient accumulation with micro-batches, this paper introduces GreedySnake, a new SSD-offloaded training system that employs *vertical scheduling*, which executes all micro-batches of a layer before proceeding to the next. Compared to existing systems that use *horizontal scheduling* (i.e., executing micro-batches sequentially), GreedySnake achieves higher training throughput with smaller batch sizes, bringing the system much closer to the ideal scenario predicted by the roofline model. To further mitigate the I/O bottleneck, GreedySnake overlaps part of the optimization step with the forward pass of the next iteration. Experimental results on A100 GPUs show that GreedySnake achieves saturated training throughput improvements over ZeRO-Infinity: 1.96 \times on 1 GPU and 1.93 \times on 4 GPUs for GPT-65B, and 2.53 \times on 1 GPU for GPT-175B. The code is open-sourced at <https://github.com/npz7yyk/GreedySnake>.

1 Introduction

Large Language Models (LLMs) have attracted widespread attention across diverse domains [5, 7, 31]. Scaling laws [16] show that LLM performance improves with increased model parameters, training data, and compute. Motivated by this trend, recent open-source LLMs such as gpt-oss [1], Qwen [3], and DeepSeek [10] often exceed 100 billion parameters. To train such large models cost-effectively, heterogeneous memory training has been proposed, where most of the training footprint resides outside GPU memory. Early systems [11–13, 18, 23, 26–28, 30, 32] leverage CPU memory, and later designs, known as *SSD-offloaded* training [20, 25, 33, 35], go a step further by storing various types of training data across both CPU memory and SSD. Without relying solely on GPU memory to host all training data, this approach offers a promising solution for LLM training under GPU memory-constrained settings. In this paper, we rethink the fundamental challenges of SSD-offloaded training and propose novel techniques that significantly improve its efficiency compared to state-of-the-art systems.

SSD-offloaded training typically offloads the large optimizer states to SSD and uses the host CPU to execute the optimizer step and update these states [20, 25]. In this setting, the optimizer step becomes the primary bottleneck due to excessive I/O: optimizer states must be loaded from SSD for updates and written back afterward, saturating the limited host-SSD bandwidth (typically a few GB/s). Jang *et al.* [15] report that this overhead can reach 80% when training GPT-2.

To facilitate data movement and reduce storage access time, prior works [20, 35] suggest deploying up to 12 SSDs or using two 4-SSD RAID0 arrays to increase host-storage bandwidth, or leveraging in-storage computing [15] to reduce storage traffic. However, these approaches require additional or specialized hardware. In practice, conventional servers are rarely provisioned with so many SSDs to scale bandwidth, making these solutions unlikely to see widespread adoption.

To tackle the optimizer step bottleneck, a common practice is to use larger batch sizes so that the optimizer step overhead—*independent* of batch size—can be amortized over an entire training iteration. Some prior works [2, 11, 20] focus on increasing the batch size within a single forward-backward pass. However, the maximum batch size is ultimately capped by the peak memory usage of the largest operator in the model, e.g., matrix multiplications in feed-forward networks. More importantly, increasing batch size causes faster growth in the data traffic for transferring *activation checkpoints* required by recomputation [6], a widely used memory-saving technique. This technique creates activation checkpoints periodically—typically at layer boundaries—during the forward pass and reconstructs intermediate activations between checkpoints in the backward pass. A larger batch size increases not only the size of each checkpoint, but also the *frequency* of checkpoints, because the amount of recovered activations between checkpoints is bounded by GPU memory capacity. These larger and more frequent checkpoints lead to *superlinear* growth in the overhead of checkpoint swapping, quickly wiping out the benefits of increasing batch size.

A fundamentally better approach to scaling batch size is *gradient accumulation* adopted by ZeRO-Infinity [25], which computes and aggregates gradients from multiple *micro-batches* within each iteration, scaling the effective batch size by increasing the number of micro-batches. Specifically, consecutive micro-batches of an iteration are executed one by

*Yikang Yue and Yishu Yin contributed equally to this work.

†Corresponding author: Xuehai Qian.

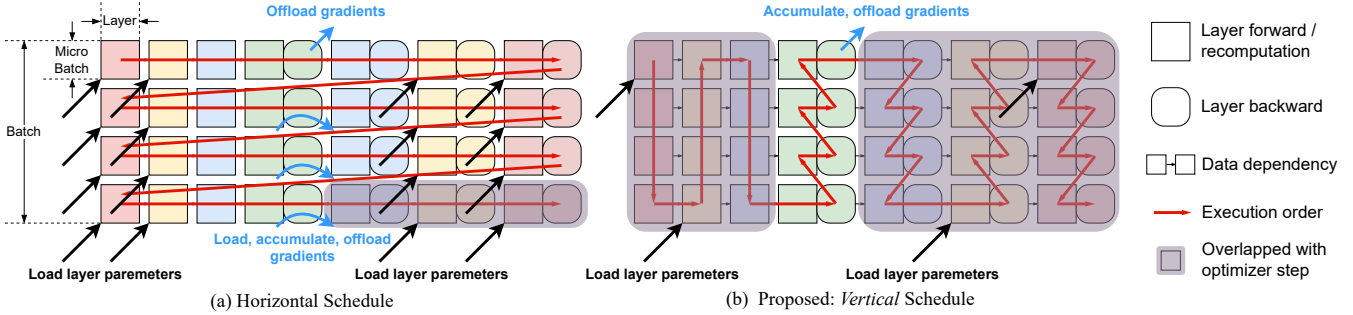


Figure 1: Gradient Accumulation: From Horizontal to Vertical. The swapping traffic is only plotted for a subset of layers.

one, and the gradients produced by each micro-batch are accumulated. However, gradient accumulation comes with its own overhead. We analyze the problem from two aspects that directly affect training performance: (1) the amount of data movement; and (2) the ability of overlapping optimizer steps with GPU computation.

Consider an N -layer LLM with total model size ms . Each training iteration processes M micro-batches under gradient accumulation, where the aggregated activation checkpoint size per micro-batch is cs . Current systems perform gradient accumulation with a *horizontal schedule* that executes micro-batches sequentially. This horizontal schedule incurs data movement between the GPU and the lower memory hierarchy from three sources: (1) loading model parameters with total size $2 \times M \times ms$, i.e., parameters are loaded for both the forward pass and the backward pass with recomputation for each micro-batch; (2) writing activation checkpoints in the forward pass and reading them in the backward pass, with total size $2 \times M \times cs$; and (3) loading, updating, and writing back gradients of all parameters across $(M - 1)$ micro-batches, leading to a total of $[2(M - 1) + 1] \times 2ms = (2M - 1) \times 2ms$ ¹. In this setting, the optimizer step can be overlapped with the backward pass of the last micro-batch for $(N - 1)$ layers.

This paper reexamines the computation schedule for SSD-offloaded training and proposes *GreedySnake*, a system based on the *vertical schedule* that executes each layer’s forward or backward computations across *all micro-batches* before advancing to the next layer. *GreedySnake* explores a key tradeoff between reduced model-parameter loading and increased activation checkpoint reads and writes. This elegant yet simple design naturally reduces overall data movement and substantially increases the amount of GPU computation that can be overlapped with the optimizer step.

On one side, the vertical schedule enables better *reuse* of loaded parameters and reduces parameter loading traffic from $2 \times M \times ms$ to $2ms$. The traffic for moving gradients is similarly reduced to $2ms$: parameter gradients from all micro-

¹We assume mixed-precision training [21]. Gradient accumulation is typically kept in full precision, so the buffer size is twice the parameter size. The first micro-batch only offloads gradients; the remaining $(M - 1)$ micro-batches fetch and offload gradients.

batches are accumulated locally in GPU memory, and the fully accumulated gradients for each layer are transferred to CPU memory only *once*. On the other hand, *GreedySnake* increases activation checkpoint traffic. Because execution switches across micro-batches at each layer, the intermediate activations of a given micro-batch are no longer kept in GPU memory when its next layer is executed; instead, they must be saved as checkpoints and later reloaded to continue the forward pass. A similar issue arises in the backward pass, where the inter-layer gradients are likewise unavailable in GPU memory when a micro-batch resumes. The *key insight* of *GreedySnake* is that parameter size scales *quadratically* with the model hidden dimension, whereas checkpoint size scales *linearly* (see Section 3.4). In other words, improving parameter reuse is more critical.

Naturally, vertical scheduling substantially increases the opportunity to overlap the optimizer step with the backward pass. Specifically, the overlapped computation becomes approximately $M \times (N - 1)$ layers of backward passes across *all micro-batches*, up from only $(N - 1)$ layers of the backward pass for *the last micro-batch*. Taking a step further, *GreedySnake* also overlaps part of the optimizer step with the forward pass of the next iteration, as long as each layer’s parameters are updated before that layer executes. By combining these two techniques, our system can ideally overlap the optimizer step with almost all GPU computation across all micro-batches, providing unprecedented tolerance to long optimizer step execution. Figure 1 compares the horizontal and vertical schedules and illustrates the benefits of the latter.

Following the roofline model of SSD-offloaded training (Figure 3), as batch size increases, training throughput initially grows under the I/O roofline and then saturates below the computation roofline. Our goal is to (i) maximize this saturated throughput and (ii) minimize the batch size required to reach it. Doing so improves algorithmic flexibility: users need not inflate batch size solely due to system constraints. In *GreedySnake*, vertical scheduling increases the highest achievable throughput, while aggressive overlap reduces the batch size required to attain it. However, both the saturation point and the batch size at which it is reached depend on

(1) how training data are distributed across GPU memory, CPU memory, and SSD, and (2) the percentage of the optimizer step to be overlapped with the forward pass of the next iteration. We formulate a linear program to automatically search this large configuration space and identify the best data-distribution and overlap ratios.

We implement GreedySnake in approximately 5K lines of Python (excluding comments and blank lines) on top of PyTorch [22] to manage computation and tensor storage, and we reuse the `asyncio`-based pipeline and the `cpu_adam` module from ZeRO-Infinity [25]. Our evaluation compares GreedySnake against ZeRO-Infinity and several other recent SSD-offloaded training systems. We run experiments on two GPU clusters and train GPT-30B, GPT-65B, and GPT-175B. The results show that GreedySnake substantially improves the saturated training throughput over all baselines.

2 Background

2.1 LLM Training Preliminaries

Vanilla LLM training. Vanilla LLM training proceeds in three stages: *forward pass*, *backward pass*, and *optimizer step*. During the forward pass, the input is propagated layer by layer, going through each layer’s parameters to generate activations. The activations produced by the last layer are used to compute the loss, while intermediate activations are retained for gradient computation. In the backward pass, the loss signal is propagated reversely through all layers, combining with stored activations produced in the forward stage to compute gradients for each parameter. Finally, in the optimizer step, parameters are updated element-wise using the parameter gradients together with optimizer states, producing updated parameters and optimizer states for the next iteration.

Pipelined optimizer step. A straightforward optimization for vanilla LLM training is to pipeline the backward and optimizer-step stages. The backward pass processes all layers in reverse order, and a layer’s corresponding optimizer step can be executed immediately after its backward pass. This technique reduces memory footprint because the gradients of those layers can be released right after their updates are applied. In addition, this pipeline is the foundation to achieve the overlapped execution of backward pass and optimizer step. Note that gradient clipping is often required for training stability [29], which necessitates computing the global L2-norm over all gradients and therefore forces the optimizer to wait until the entire backward pass completes. Recent work breaks this dependency via speculative optimizer steps [18], exploiting the observation that gradient clipping rarely modifies gradients in practice.

Mixed precision training. It accelerates forward and backward computation by leveraging lower-precision arithmetic [21], a common practice adopted in industrial training pipelines [10, 29]. During the forward pass, inputs and

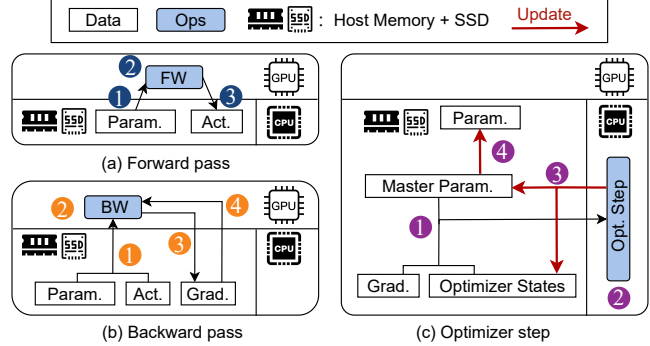


Figure 2: A conceptual diagram of the heterogeneous memory LLM training. Overview of (a) the forward pass, (b) the backward pass, and (c) the optimizer step.

full-precision parameters (termed *master* parameters) are cast into lower-precision formats (commonly FP16 or BF16, with recent exploration of FP8 and other quantized variants) as they propagate through the layers. To preserve numerical stability, selected values such as the loss and certain intermediate activations are retained in full precision. During the backward pass, gradients are computed in reduced precision, while critical accumulations are promoted to full precision. Finally, in the optimizer step, gradients are scaled and combined with higher-precision optimizer states (typically FP32, though BF16 has recently been explored) to update the master parameters and optimizer states.

Activation checkpointing. This memory-saving technique trades additional computation for reduced storage of intermediate activations [6]. Rather than retaining all activations from the forward pass, it saves only a subset as *checkpoints* and discards the rest. During backpropagation, before computing gradients for layers between two consecutive checkpoints, the system *recomputes* the missing activations by replaying the forward pass starting from the nearest checkpoint, and then runs the backward pass using the reconstructed activations. This enables training deeper models or larger batch sizes within the same memory budget.

Gradient accumulation. Designed to reduce the effective memory footprint of training, it decomposes the computation of a large batch across multiple smaller *micro-batches* with multiple forward and backward passes. The gradients produced by all micro-batches are accumulated in full precision, and then the optimizer step is applied to update the parameters. This approach allows training with larger effective batch sizes than would otherwise fit into GPU memory, while preserving the statistical benefits of large-batch optimization.

2.2 SSD-Offloaded Training

Figure 2 provides an overview of SSD-offloaded LLM training methods with mixed-precision computation, under the

assumption that most training data, including model parameters and optimizer states, must be offloaded. In this setting, per-layer activation checkpointing (i.e., checkpointing the input activations of all Transformer blocks) is typically applied for two reasons. First, it reduces activation-swapping traffic by limiting it to the swapping of only inter-layer checkpoints, rather than all activations. Second, it ensures that GPU memory only needs to accommodate the footprint of a single Transformer layer’s backward pass at a time, thereby enabling the system to train with larger batch sizes or bigger models. The detailed data traffic is explained as follows.

In the forward pass (Figure 2(a)), the GPU loads the low-precision parameters of an LLM layer (1), conducts the layer’s forward computation (2), and offloads its input activations as the checkpoint (3). The system iteratively performs steps 1–3 over all layers, which can be overlapped via pipelining in practice.

In the backward pass (Figure 2(b)), GPU loads the mixed-precision parameters and checkpointed activations of an LLM layer (1), conducts the layer’s backward computation (2), and offloads the resulting gradients (3). When gradient accumulation is enabled, accumulated gradients are fetched before the upcoming backward computation of the same layer (4) to accumulate new gradients. This sequence repeats for all layers in reverse order and can also be overlapped.

When all forward and backward passes are finished, the system performs optimizer steps (Figure 2(c)) for each parameter chunk: the CPU loads the chunk’s gradients, master parameters, and optimizer states (1), conducts the optimizer step (2), and updates the master parameters and optimizer states (3). The master parameters are then converted into low precision to update the low-precision parameters (4). This sequence repeats for all parameter chunks, and the forward pass of the next iteration begins after all updates are completed. The chunk granularity need not align with layer boundaries, since the optimizer step is inherently element-wise.

Since the master parameters are only involved in optimizer step, we treat them as part of the optimizer states for the remainder of this paper. Unless otherwise specified, we assume the training optimizer to be Adam [17]. Each model weight element is therefore associated with three full-precision states, i.e., master parameter, momentum, and variance. For clarity, “*parameter*” in the subsequent discussion denotes the low-precision version used in forward and backward passes.

3 SSD-Offloaded Training Scheduling

3.1 Roofline Model

For simplicity, we assume that optimizer states are entirely stored in SSD. Therefore, each training iteration must load the optimizer states from the SSD once and write them back once, establishing a fundamental I/O bound.

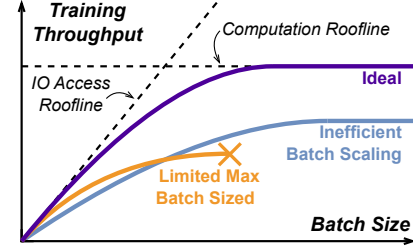


Figure 3: Roofline model of SSD-offloaded Training

Figure 3 presents a roofline model for SSD-offloaded training, where the x- and y-axis represents batch size and training throughput. Two performance bounds constrain the achievable throughput. First, the *I/O access roofline*—a line passing through the origin—represents the scenario where iteration time equals the storage access time for optimizer states. No system can exceed I/O access roofline without reducing per-iteration I/O volume. Second, the *computation roofline*—a horizontal line—represents the maximum throughput achievable when GPU compute capacity becomes the bottleneck, independent of batch size or memory constraints.

Ideally, an SSD-offloaded training system should first exhibit near-linear throughput scaling with batch size, close to the IO access roofline, when optimizer state’s I/O access time dominates iteration time, then rapidly converge to the computation roofline. At this point, the system achieves throughput comparable to training without offloading, effectively hiding all I/O overhead.

However, existing systems exhibit two suboptimal modes. The first mode suffers from *limited maximum batch size*: architectural constraints prevent sufficient batch size scaling, and the overhead of scaling remains so high that even at maximum batch size, throughput remains far below the computation roofline. The second mode, while supporting arbitrarily large batch sizes, demonstrates *inefficient batch scaling*: high batch size scaling overhead and an inability to effectively overlap optimizer computation with GPU execution cause throughput to increase slowly and converge prematurely below the computation roofline.

3.2 Single Forward-Backward Schedule

A group of SSD-offloaded training systems is explicitly designed and optimized for a single forward-backward pass execution [11, 20, 30]. To boost the training throughput, the common strategy employed is to maximize the training batch size in a single forward-backward pass. With recomputation, the size of the recovered activations between checkpoints is bounded by GPU memory capacity. To accommodate enlarged operation with increased batch size, checkpoints have to be created more frequently and carefully swapped. For example, recent work [20] additionally checkpoints the activa-

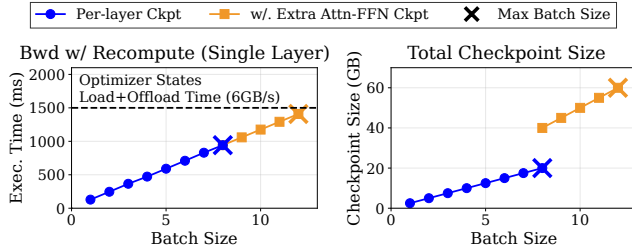


Figure 4: Batch size scaling in single forward-backward schedule. We use GPT-65B (Section 6.1) as an example.

tion between the attention layer and the feed-forward network (FFN) inside each Transformer block [31].

As shown by Figure 4, even with such optimizations, the maximum reachable batch sizes are typically not large enough to entirely hide the optimizer step. From an implementation perspective, we admit that by further optimizing such activation checkpointing and swapping [4, 14, 34], the maximum achievable batch size may be further increased. However, we consider scaling the batch size for a single forward-backward pass ineffective for two fundamental reasons.

First, the most memory-intensive operation in the training computation graph fundamentally caps the maximum achievable batch size. Second, when increasing the frequency of activation checkpointing to achieve a larger batch size, the total traffic increases superlinearly because not only more tensors are swapped, but also the swapped tensors become larger along the batch dimension. Essentially, this approach increases the batch size *at an exceedingly high cost*. As shown in Figure 4, compared to per-layer activation checkpointing, applying extra checkpoints between the attention layer and the feed-forward network can only lead to a 1.5x improvement in the maximum achievable batch size. However, this in turn exacerbates the checkpoint swapping traffic by a factor of 3x, because the extra checkpoints first double the traffic under the same batch size, and the batch size increases by a factor of 1.5x, which jointly leads to the inflation. Note that an increase in checkpoint size from 20GB to 60GB for one GPU will be inflated much more drastically when extended to data-parallel training with multiple GPUs. For example, with 4 GPUs, it will lead to an overwhelming 240GB for checkpoints, forcing a higher percentage of—or even almost all—remaining training data to be offloaded to SSD, which consequently leads to higher SSD traffic.

3.3 Horizontal Gradient Accumulation

An alternative approach to scaling the training batch size is to increase the number of forward-backward passes, rather than scaling the batch size for a single forward-backward pass. This method scales the aggregated batch size by scaling the number of passes with multiple micro-batches. The computa-

tional schedule for gradient accumulation in existing systems, such as ZeRO-series [24, 25, 27], is shown in Figure 1(a). We refer to this schedule as *horizontal* gradient accumulation, in which the system performs the forward and backward passes of all layers for one micro-batch before moving on to the next. This solution works well in pure GPU memory training, since for each micro-batch, the activation checkpoints created in the forward pass can be directly used in the backward pass. It effectively ensures a constant peak GPU memory usage that does not scale with the number of micro-batches.

However, we find the horizontal schedule ineffective for SSD-offloaded training for two key reasons. First, in the horizontal schedule, for each micro-batch, the total low-precision parameters have to be loaded to GPU(s) twice, once during the forward pass and once during the backward pass since recomputation requires the model weights (see Section 2.1). Additionally, for each micro-batch during the backward pass, the buffer for accumulating full-precision gradients must be loaded onto the GPU(s), and written back after accumulation. These requirements significantly increase the memory traffic between GPU and host CPU memory, and the impact will be even larger if the low-precision parameters or the full-precision gradients have to be offloaded to SSD.

Second, though the batch size can be scaled as needed, the portion of GPU compute that can be overlapped with the optimizer step remains unchanged. This is because the optimizer step can start only after the last micro-batch completes the backward pass of the last layer and the accumulated parameter gradients have been transferred to CPU memory. Besides, the common convention [11, 18, 20, 35] assumes that the model is fully updated before the start of the next iteration. As a result, at most the backward pass over all layers of a single micro-batch can be overlapped with the optimizer step, and this overlap does *not* scale even if we increase batch size by using more micro-batches. The gray box in Figure 1(a) shows the computation that can be overlapped with the optimizer states. It lead to the premature saturation of training throughput when training with horizontal gradient accumulation schedule.

3.4 Proposed: Vertical Gradient Accumulation

We propose *vertical* gradient accumulation scheduling (interchangeable with vertical scheduling), a simple yet elegant solution to overcome the inefficiencies of horizontal schedule. Instead of completing all layers of one micro-batch before moving onto the next, vertical scheduling performs the forward or backward computation of a specific layer across *all micro-batches* before moving to the next layer, as shown by Figure 1(b). This schedule improves parameter reuse and avoids the swapping of gradient accumulation buffers. Specifically, multiple micro-batches can share the parameters of the same layer, rather than loading them repeatedly. Similarly, the gradient-accumulation buffer can remain resident in GPU memory while aggregating gradients across all micro-batches,

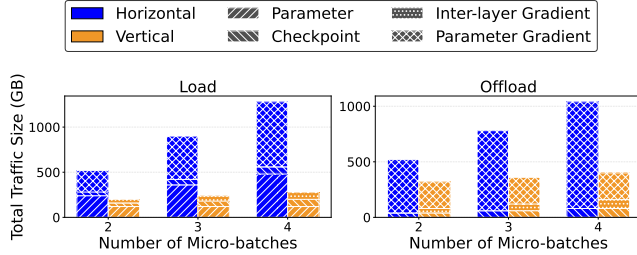


Figure 5: Impact of horizontal vs. vertical scheduling on GPU load and offload traffic. We use GPT-65B as an example.

eliminating the need to swap the buffer in and out.

Moreover, vertical schedule also significantly increases the opportunities to overlap the optimizer step with GPU compute. In particular, with the backward computation finishing vertically for each layer for all micro-batches, the optimizer step can be overlapped with the backward computation of all micro-batches for almost all layers (except the last, which is processed first in backward); and with elaborate implementation, be even overlapped with part of the forward pass. Figure 1(b) indicates the clear increase of overlapping opportunities with vertical schedule.

It is worth noting that vertical schedule is not a “free” lunch. Compared to the horizontal schedule, now the system has to switch between different micro-batches. This requires the GPU to offload the output activations of each micro-batch for every layer during the forward pass, which will be later needed as the input for (1) the next layer in forward pass, and (2) the recomputation of the same layer in backward pass. Therefore, this schedule essentially trades extra checkpoint swapping for the reduced parameter loading and gradient swapping traffic. *Is the tradeoff really beneficial?*

We claim the answer is YES because the two traffic scales differently with the model’s hidden dimension: (1) the number of elements in each inter-layer activation checkpoint only scales *linearly* with the model’s hidden dimension; and (2) the number of elements in each LLM layer scales *quadratically*—mainly due to the projection matrices in FFNs. Therefore, the size of each activation checkpoint is typically smaller than the size of each LLM layer.

For an LLM in tens of billions scale or more, parameter reusing should be prioritized over activation checkpoints. For example, when training a GPT-style 65B model with a micro-batch size equals 8 and sequence length equals 2048 (see Section 6.1), the number of elements in each inter-layer activation checkpoints is $8 \times 2048 \times 8192 \approx 1.34 \times 10^8$ while the number of parameters per LLM layer is approximately 8.05×10^8 , which is 6× as large. As shown in Figure 5, adopting vertical schedule instead of horizontal schedule dramatically reduces both GPU load and offload traffic, primarily thanks to the reduction of the swapping traffic for parameters and gradients by a factor close to the number of micro-batches.

4 Pipelined Vertical Scheduling

This section discusses the detailed pipelined execution of forward pass, backward pass, and optimizer step with vertical scheduling. We focus on two design goals: (1) excellent utilization of various system resources, i.e., GPU/CPU computing and memory, communication bandwidth between CPU and GPU, as well as between CPU memory and SSD; and (2) efficient overlapping of various operations to mitigate the large storage-access overhead and optimize performance.

4.1 Problems and Principles

While the idea of vertical scheduling is intuitive, realizing it efficiently requires delicate considerations. First, we need to determine the granularity of data transfer to maximize overlapping opportunity. Second, with the execution of different tasks being conducted concurrently, we need to carefully determine the time to initiate the necessary operations, to *get the right data at the right time*. Third, the system should eliminate the pipeline bubbles as much as possible. To solve these problems, GreedySnake follows three *design principles*:

Differentiated data movement granularity. The data traffics between GPU and CPU memory are different from those between CPU memory and SSD. To ensure efficient storage I/O, the system performs data transfer between SSD and CPU memory with larger layer granularity. To align with the fact that computation and data fetch in GPU are performed at micro-batch granularity, data between CPU and GPU memory is transferred with smaller micro-batch granularity, which means that the transferred data is divided into pieces equal to the number of micro-batches. Based on this principle, between CPU and GPU memory, layer parameters are transferred in micro-batch granularity, even if they logically belong to one layer; between SSD and CPU memory, activation checkpoints of all micro-batches for a layer are transferred together, even if they are logically independent.

Reversely determined operation scheduling. Different kinds of computation, i.e., forward, backward pass, and optimizer step, depend on different inputs stored in various locations, i.e., GPU/CPU memory or SSD, with different cost of data transfer. To ensure the required data is available at the right time in the right place, we infer the time to initiate data transfer reversely starting from the computation where the data is needed. As shown later, this leads to a compact and efficient pipeline schedule.

Automated configuration space exploration. Based on the roofline model in Figure 3, GreedySnake aims to achieve the highest training throughput with a minimal batch size. To achieve the near ideal setting, a huge configuration space, e.g., the ratios of activation checkpoints, parameters, and optimizer states to be stored in CPU memory and SSD, needs to be searched, making it impractical to perform manually. We employ a simple yet accurate performance model to pre-

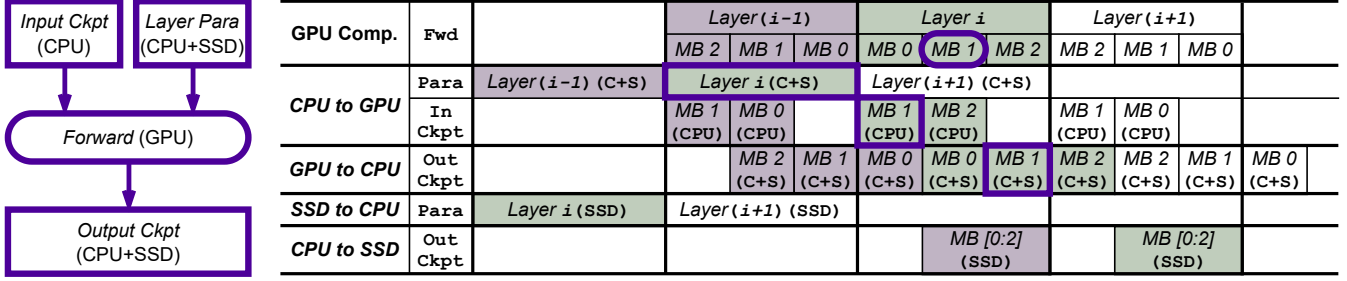


Figure 6: The forward dataflow in GreedySnake (left) and its pipelined version (right).

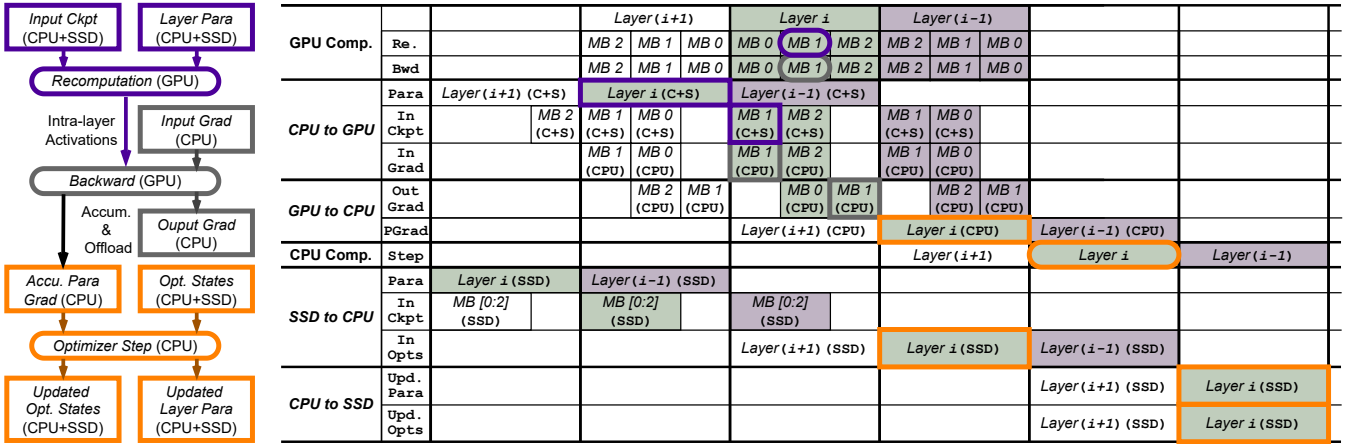


Figure 7: The optimizer-backward overlapping dataflow in GreedySnake (left) and its pipelined version (right).

dict the forward and backward execution time of a single LLM layer. We then employ linear programming to minimize the combined execution time of forward, recomputation, and backward, under a given memory constraint.

4.2 Forward Pass

Figure 6 shows the pipelined execution of three consecutive layers with three micro-batches for forward pass. The computation graph shows that, the forward pass depends on two inputs: activation checkpoints and layer parameters. The input checkpoints produced by the previous layer are written to the SSD but at the same time cached in CPU memory to be consumed by the current layer. The layer parameters and output checkpoints are stored in both SSD and CPU memory.

Each *pipeline stage* performs the forward computation of a layer after all parameters are loaded into GPU memory. Based on the first design principle, the checkpoints of micro-batches for this layer are loaded one by one with a pipeline within the stage. It is illustrated by MB0, MB1, and MB2 below ‘Layer i’ and the overlapped CPU-to-GPU transfer, e.g., during the execution of MB0, the checkpoint of MB1 is loaded into GPU. Note that the first micro-batch MB0 does not need to load the checkpoint, as long as we ensure consecutive layers *alternate* between opposite micro-batch execution order, e.g.,

Layer (i-1) follows the order MB2 → MB1 → MB0, and Layer i follows the order MB0 → MB1 → MB2. In this way, the checkpoint produced by MB0 of Layer (i-1) can be kept in GPU memory and directly used by MB0 of Layer i. After a micro-batch, the output checkpoints are stored to CPU memory and SSD. For the CPU portion, the data are directly written to the target memory address; for the SSD portion, the data of each micro-batch are first collected in a buffer in CPU memory, and then written to SSD when all micro-batches are completed, shown as MB[0:2] (SSD). This SSD offloading is performed in the next pipeline stage, overlapped with the forward pass of Layer (i+1).

Next, we consider parameter transfer, which is performed in two steps. To ensure the availability of parameter in GPU memory for Layer i’s forward pass, the first step—transfer parameters in SSD to CPU—is initiated *two* pipeline stages in advance. It is the *latest* time to schedule it without introducing wait for forward pass. After that, during exactly *one* stage before Layer i’s forward pass, the second step—transfer parameters from CPU to GPU memory—is scheduled, fully overlapped with the execution of Layer (i-1)’s forward pass. Again based on first design principle, the layer’s parameters are transferred in multiple chunks equal to the number of micro-batches for better efficiency.



Figure 8: The optimizer-forward overlapping dataflow in GreedySnake (left) and its pipelined version (right).

4.3 Overlap Backward with Optimizer Step

Figure 7 shows the pipelined execution of backward pass of Layer (i-1), Layer i, and Layer (i+1), and how the optimizer step is performed after Layer i’s backward pass. The computation graph shows the combined data dependence of backward pass and optimization step. First, all intra-layer activations are recovered by recomputation using input checkpoints produced during forward pass and layer parameters, both are stored in CPU memory and SSD. The backward pass depends on: (1) input inter-layer gradients stored in CPU memory produced by the previous backward layer; and (2) all activations produced by recomputation. The output of the backward pass by one micro-batch includes the output inter-layer gradients passed to the next layer, and the parameter gradients accumulated in GPU memory, which are transferred to CPU memory after all micro-batches of a layer are finished. The inter-layer gradients are passed between layers through CPU memory, similar to the inter-layer activation checkpoints in forward pass, except that they are not written to SSD.

After all micro-batches of a backward layer are completed, the CPU optimizer step is executed based on the fully accumulated parameter gradients and optimizer states partially transferred from SSD. It generates updated layer parameters and optimizer states, both will be stored in CPU memory and SSD. In the following, we explain how the computation graph is realized in GreedySnake.

Consider Layer i, the recomputation is divided into micro-batches, but does require the whole parameter of the layer. Similar to forward pass, they are transferred in two steps scheduled in two earlier pipeline stages. Since the input checkpoint can be transferred to GPU memory in micro-batch granularity, the SSD-to-CPU memory transfer of this data in layer granularity, i.e., MB[0:2] (SSD), is scheduled in *one* pipeline stage earlier than Layer i’s backward computation. It is because by the end of that stage, only the input checkpoint of MB0 needs to arrive in GPU memory. That of MB1 and MB2 are transferred within Layer i’s backward computation stage from CPU memory with an in-stage pipeline, similar to checkpoints in forward pass.

After MB-i’s recomputation is finished, MB-i’s backward computation depending on the output of recomputation and

input gradients can start. Note that while MB-i of recomputation and backward are placed during the same time period, dependence exists between them, we draw the figure this way to keep it clean without introducing much confusion. The input gradients’ behavior is essentially the same as checkpoints of forward pass between layers: Layer i reads them in micro-batch granularity from CPU memory. Moreover, input gradients are directly forwarded through GPU memory between the two micro-batches before and after layer boundary.

Next we consider optimizer step executed on CPU. The parameter gradients of Layer i are accumulated across all micro-batches in GPU during computation, in the next pipeline stage, they are transferred to CPU memory. In the same stage, the SSD portion of Layer i’s optimizer state is transferred from SSD to CPU memory. After both accumulated parameter gradients and optimizer states are available in CPU memory, the optimizer step is performed in the following pipeline stage. Finally, part of the updated parameters and optimizer states are written to SSD, in the rightmost pipeline stage. All these five key steps are highlighted with orange boxes.

4.4 Overlap Optimizer Step with Forward

While vertical scheduling increases the potential of overlapping optimizer step, moving the optimizer states between SSD and CPU memory still incurs considerable overhead. Consequently, as the number of micro-batches increases and the system shifts from I/O-bound to compute-bound (see Section 3.1), the forward pass becomes compute-bound first, while the backward pass remains I/O-bound, because the I/O-intensive optimizer step is overlapped with it.

To improve this obvious suboptimality and spread I/O operations over longer period, our main insight is to *delay certain percentage of optimizer step to the forward pass of the next iteration*. We quantify the portion of optimizer step to be delayed by defining the *delay ratio* $\alpha \in [0, 1]$. It also means, for each layer, only $(1 - \alpha)$ of optimizer states and parameters are updated in the backward pass. As a result, the CPU-SSD traffic of optimizer states by the end of the current iteration is reduced by α , and the reduced traffic is added to the forward pass of the next iteration.

Delaying α of optimizer step to the next iteration also requires keeping the accumulated gradients longer, requiring extra CPU memory. However, straightforward designs will likely offset much of the benefits of this optimization: offloading α of gradients to SSD by itself incurs additional SSD traffic, defeating the initial purpose; while allocating extra CPU memory for these gradients negatively affects performance since such memory would have been otherwise used to host offloaded training states. In GreedySnake, we made an effort to enable the delayed optimizer step execution *without increasing memory consumption*.

The key insight is to *reuse* the CPU memory allocated for offloaded parameters and checkpoints, both of which remain resident throughout training. Layer by layer during the backward pass, the corresponding data in such memory becomes obsolete gradually. To be specific, the CPU-offloaded parameters become obsolete after recompute, after the partial optimizer step, α of them remain stale and can be reclaimed to store gradients. Similarly, checkpoints also become obsolete after recompute and the memory can be reused as well. Our implementation requires that the gradient memory needed for the delayed optimizer step do not exceed the combined capacity of these two reclaimed memory resources. After the remaining α fraction of optimizer step completes, the reclaimed parameter buffers are overwritten with the corresponding *updated* parameters, bringing all CPU-resident parameters up to date.

Figure 8 shows the pipelined execution of partially delayed optimizer step and forward pass. The computation graph is slightly changed to link the α updated layer parameters to forward pass of the next iteration that depends on them. Consider Layer i , α of the optimizer states used for the delayed execution is transferred from SSD to CPU memory, *three* stages ahead of Layer i ’s forward pass. In the next stage, the CPU optimizer step is performed, producing the updated α fraction of parameters in CPU memory. To ensure all updated parameters are available in CPU memory before CPU-to-GPU prefetching, the transfer of the $(1 - \alpha)$ fraction of parameters from SSD to CPU is scheduled in the same pipeline stage—two stages ahead of Layer i ’s forward pass. Afterward, they can be sent together from CPU to GPU memory, in the stage right before Layer i ’s forward pass. Besides, the updated parameters and optimizer states are written back to SSD, bringing all SSD-resident states up to date. In Figure 8, the above key steps are highlighted with orange boxes (part of optimizer step) and purple boxes (part of forward pass).

4.5 LP-based Configuration Search

We formulate the configuration selection as a small Linear Programming [8] (LP) process. The overall procedure is summarized in Algorithm 1. The goal of the algorithm is to find the smallest micro-batch count n that reaches the saturated training throughput and to record the corresponding step de-

lay ratio α and storage ratios x for system configuration. As shown, the algorithm first benchmarks the target machine and packs the results into system parameters \mathcal{M} . This includes GPU/CPU memory, SSD bandwidth, forward/backward time and other system metrics. Then, the algorithm searches over micro-batch count n (loop) and step delay ratio α (argmax). For each $n - \alpha$ pair, the algorithm will build a small LP to find the optimal storage ratio for checkpoints, parameters and optimizer states (gradients are 100% stored in CPU). Assuming that SSD traffic time and computation can always overlap, we consider their maximum as the effective forward/backward time. Then, the objective function will minimize per-layer iteration time with a regularization penalty to minimize SSD traffic when possible. While other constraints are considered in developing the algorithm, only three become active at the decision boundary: CPU memory capacity, GPU computation time, and SSD bandwidth. With these constraints considered, we ensure that all data fits in the available CPU memory, and that the projected iteration time correctly reflects forward/backward passes overlapped with optimizer steps. By solving this LP, the algorithm identifies the configuration that delivers the highest training throughput for each (n, α) combination. It continues to increase n until throughput stops improving and saturated. This approach can also estimate the overall iteration time and throughput of the entire model, i.e., per-layer time multiplied by the number of layers, plus time for embedding, LLM heads, and other components.

5 System Implementation

GreedySnake is implemented in approximately 5K lines of Python (excluding comments and blank lines) based on PyTorch [22] to manage computation and tensor storage, with the `asyncio` and `cpu_adam` module reused from ZeRO-Infinity [25]. To efficiently scale the computation, ZeRO-style Fully Shared Data Parallellsim [24, 36] (FSDP) is integrated. To implement the pipelined execution based on vertical scheduling discussed in Section 4, we implement three coordinators to manage different types of training data.

The first is *Inter-layer Tensor Coordinator*, which is responsible for the data movement of activation checkpoints in forward pass and inter-layer gradients in backward pass. The two types of data share similar access patterns during execution. The second is *Parameter Coordinator*, which is responsible for fetching parameters. The last is *Optimizer Step Coordinator* that is responsible for orchestrating data movements of other data types, including optimizer states and parameter gradients. The pipelined execution discussed before can be considered as a two-dimensional resource-time space. The coordinators focus on the *resource dimension*: they together ensure that the correct set of operations are scheduled for each pipeline stage, i.e., a period in time dimension.

Figure 9 provides an example of operations of parameter coordinator in various components. At the given time, it

Algorithm 1: Global Configuration Optimizer

```

Input : System parameters  $\mathcal{M}$ 
Output : Optimal micro-batch count  $n^*$ ,  $\alpha^*$ , and storage ratios  $\mathbf{x}^*$ 
1 Function SOLVECONFIG( $\mathcal{M}$ ,  $n$ ,  $\alpha$ ):
2    $\mathbf{x} \in [0, 1]^3$            // For ckpt, param and opt states
3    $t_f \leftarrow \max(\mathcal{M}.\text{fwd\_compute\_time} \times n, \text{get\_fwd\_ssd\_time}(\mathcal{M}))$ 
4    $t_b \leftarrow \max(\mathcal{M}.\text{bwd\_compute\_time} \times n, \text{get\_bwd\_ssd\_time}(\mathcal{M}))$ 
5    $\text{LP} \leftarrow \text{new LpProblem}$ 
6    $\text{LP} += \text{get\_cpu\_mem}(\mathcal{M}, \mathbf{x}) \leq \mathcal{M}.\text{usable\_dram}$ 
7    $\text{LP} += \text{minimize}(t_f + t_b)$            //  $t_b$  includes recompute time
8   if  $\text{LP}$  is feasible then
9     return  $(\mathbf{x}, t_f + t_b)$            // storage ratios and iteration time
10  else
11    return  $(\text{None}, \infty)$ 
12
13 Function FINDOPTIMALCONFIG( $\mathcal{M}$ ):
14    $\text{max\_throughput} \leftarrow 0$ ,  $\text{best\_config} \leftarrow \text{None}$ 
15    $n \leftarrow 0$ ,  $\mathcal{A} \leftarrow \{0.01, 0.02, \dots, 0.50\}$ 
16   while true do
17      $n \leftarrow n + 1$ 
18      $\alpha^* \leftarrow \arg \max_{\alpha \in \mathcal{A}} \frac{n}{\text{SolveConfig}(\mathcal{M}, n, \alpha).\text{iteration\_time}}$ 
19      $\text{result}^* \leftarrow \text{SolveConfig}(\mathcal{M}, n, \alpha^*)$ 
20      $\text{throughput}^* \leftarrow \frac{n}{\text{result}^*.\text{iteration\_time}}$ 
21     if  $\text{throughput}^* \geq 1.01 \times \text{max\_throughput}$  then
22        $\text{max\_throughput} \leftarrow \text{throughput}^*$ 
23        $\text{best\_config} \leftarrow \text{result}^*$ 
24     else
25       break
26
27   return  $\text{best\_config}$ 

```

orchestrates the parameter fetching for *three* layers. Layer (i+2)'s parameters are fetched in layer granularity from SSD to CPU memory; Layer (i+1)'s parameters are transferred from CPU memory to GPU memory in micro-batch granularity, i.e., the transfer of a whole layer is divided into pieces equal to the number of micro-batches; and Layer i's parameters are currently in GPU memory used by computation. With two GPUs, each piece of parameter in GPU will be generated by the all-gather operation. We choose to transfer parameters in micro-batch granularity for performance reason. Due to the interference between the checkpoint traffic from GPU to CPU and the parameter traffic from CPU to GPU, transferring all parameters together prevents the utilization of the full communication bandwidth between CPU and GPU. The issue is largely resolved when the transfer of different data types are divided into the *same* micro-batch granularity.

Each coordinator allocates various CPU buffers that should be pinned in CPU memory to support efficient asynchronous data movement. However, as of the recent PyTorch (Version: 2.9.1+cu128), individual requests for allocating pinned memory buffer are padded to buffers of power-of-two sizes, leading to a waste of at most half of the allocated memory. GreedySnake typically allocates buffers of the same size, e.g.,

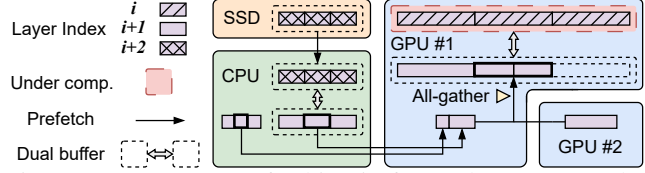


Figure 9: Parameter prefetching in forward pass across the memory hierarchy. We use #GPU=2, #MB=3 as an example.

Table 1: Configurations of the evaluation servers

	Machine 1	Machine 2
CPU	Dual EPYC 7302 16-Core	Dual Xeon Platinum 8462Y+
Mem.	256 GB 3200MHz DDR4	400 GB 3200MHz DDR4
PCIe	PCIe Gen 4	PCIe Gen 4
GPU	NVIDIA A5000 (24GB)	NVIDIA A100 (40GB)
SSD	PM9A3 3.84TB NVMe	4TB Cloud Storage
CUDA	V12.1.105	V12.8.93
PyTorch	2.5.1+cu121	2.8.0+cu128

the CPU checkpoint buffer for all micro-batches and layers. Based on this pattern, we use dynamic programming to find the set of power-of-two buffers that can hold a given number of buffers of certain size with minimum wasted memory.

6 Evaluation

6.1 Evaluation Setup

Evaluated Machine. We perform all the experiments on two servers whose configurations are summarized in Table 1.

Workloads. Same as related work [11, 20, 25], we use GPT-style LLMs provided by Megatron-LM [29]. The model configuration is shown in Table 2.

Baseline Configurations. We compare GreedySnake against the following open-sourced SSD-offloaded training frameworks: (1) *ZeRO-Infinity* [25]: A widely deployed, production-grade SSD-offloaded training framework that optimizes memory management through coordinated prefetching and computation-communication overlap. We enable activation checkpointing with CPU memory offloading to maximize per-pass batch size. Parameters and optimizer states are offloaded to SSD by default, while parameters are retained in CPU memory when capacity permits to reduce I/O overhead. (2) *Ratel* [20]: An SSD-offloaded training system that co-designs fine-grained activation checkpointing with checkpoint swapping across the memory hierarchy. We reuse the original open-source codebase for single-GPU training; for multi-GPU training, we extend it with FSDP on a best-effort basis. (3) *TeraIO* [35]: An SSD-offloaded training system that optimizes data movement through tensor lifetime analysis. Because the open-source codebase does not support activation checkpointing and is coupled with TorchTitan [19], we use its tensor lifetime profiler to analyze ZeRO-Infinity execution traces and report the throughput projected by the framework's analyzer under the optimized tensor offloading

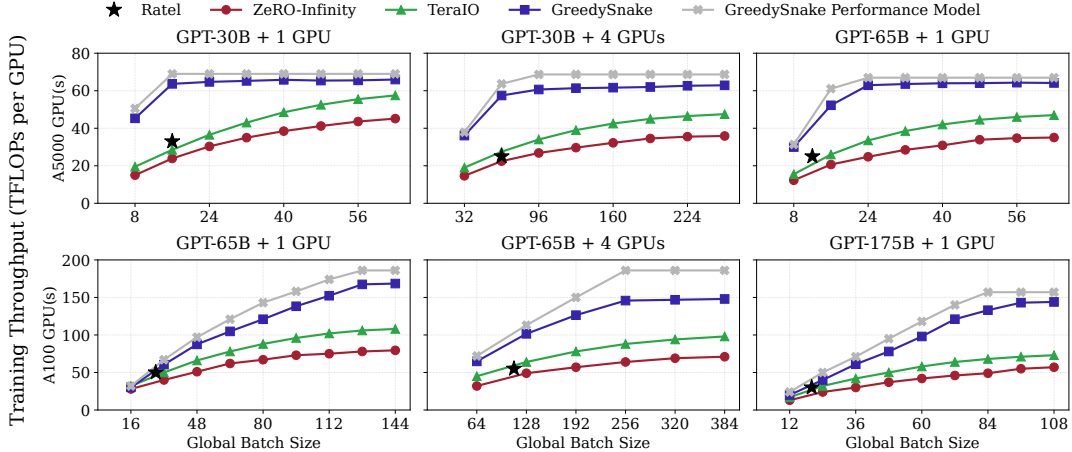


Figure 10: End-to-end throughput of SSD-offloaded training systems when training GPT-style LLMs with sequence length 2048.

Table 2: Model configuration in evaluation.

Model Size	#Layers	#Heads	Hidden Dimension
30B	48	56	7168
65B	80	64	8192
175B	96	96	12288

and prefetching plan. We confirmed this methodology and the produced numbers with the authors to ensure an accurate representation of the system’s capabilities. This baseline represents a highly optimized, horizontally scheduled gradient-accumulation scheme with effective tensor management.

6.2 End-to-End Throughput Comparison

Figure 10 shows the end-to-end throughput with different global batch sizes of GreedySnake compared to the other systems. In the smaller A5000-cluster, we train GPT-30B with 1 and 4 GPUs, and GPT-65B with 1 GPU. In the larger A100-cluster, we follow a similar practice but with larger models: training GPT-65B with 1 and 4 GPUs and GPT-175B with 1 GPU. Both ZeRO-Infinity and Ratel fail to support the $4 \times$ A5000-65B and $4 \times$ A100-175B configurations due to severe CPU memory fragmentation. In contrast, GreedySnake successfully trains under these settings, so we omit the corresponding figures. We report that, on GreedySnake, training GPT-65B and GPT-175B with 4 GPUs across the two clusters achieves 63.1 and 128.3 TFLOPs per GPU, respectively.

For both ZeRO-Infinity and GreedySnake, we choose the largest possible micro-batch size the system can support. It is the most favorable choice for ZeRO-Infinity: as the representative system using gradient accumulation with horizontal scheduling, larger micro-batch size is better because it can reduce the parameter loading cost. The global batch size is generated by increasing the number of micro-batches based on the chosen size for ZeRO-Infinity. For example, for GPT-30B on the A5000-node, the largest batch size for ZeRO-Infinity is 8, and we use 8, 16, 24, ..., 64 as the global batch size.

We choose the largest global batch size when GreedySnake’s throughput is saturated and well beyond the shifting point from I/O-bound to compute-bound.

For GreedySnake, the micro-batch size is much smaller, typically 1 or 2, because the system allocates more memory to support the pipeline, e.g., two copies of the gradients are required in GPU memory for “vertical” accumulation across micro-batches. Based on the micro-batch size, the percentage of data distribution among SSD and CPU memory, and the delay ratio are determined by LP-based configuration search. Since LLM training is compute-bound, even the smaller micro-batch size can well utilize the compute resource. In this sense, GreedySnake offers a new way to devote the memory resource to support efficient pipelined execution: using small but enough micro-batch sizes. In contrast, ZeRO-Infinity prevents this possibility since small micro-batch size will directly lead to a significant increase of traffic for moving parameters. Compared to ZeRO-Infinity, the result convincingly shows that GreedySnake achieves much higher throughput with much smaller global batch size, indicating a significant advance over the state-of-the-art. Overall, compared to ZeRO-Infinity, GreedySnake improves saturated throughput by $1.96 \times$ and $1.93 \times$ on 1 and 4 A100 GPUs for GPT-65B, and by $2.53 \times$ on 1 A100 GPU for GPT-175B.

Among the other systems, Ratel exemplifies scaling batch size within a single forward-backward schedule. For each configuration, we report only the largest batch size that the system can support. As discussed earlier, this approach fails to scale the global batch size, and the resulting throughput remains well below saturation. These results provide clear evidence that the single forward-backward regime is fundamentally unsustainable. At the same global batch size, we observe that Ratel performs slightly better than ZeRO-Infinity because Ratel (1) overlaps the backward pass with the optimizer step, and (2) prefetches parameters layer by layer, whereas ZeRO-Infinity does not assume the model consists of uniform layers. The second factor enables a more uniform and

compact prefetching pipeline in Ratel. We also find that Ratel’s advantage over ZeRO-Infinity diminishes with 4 GPUs, because checkpoint sizes increase with data parallelism, forcing the system to devote substantially more CPU memory to store checkpoints.

TeraIO focuses on analyzing the lifetime of each tensor to generate better offloading and prefetching plan based on the tensor access pattern obtained with profiling. We apply this methodology to the tensor access trace of ZeRO-Infinity, and observe that the throughput of the optimized execution is higher than ZeRO-Infinity and scales slightly better with global batch size. On the one hand, the result shows the potential for tensor lifetime analysis. On the other hand, the smaller improvements over ZeRO-Infinity compared to the larger gap from GreedySnake indicate the limitations of the “local” optimization: without changing the inefficient horizontal global scheduling, the potential of throughput improvement is relatively small. In fact, this result indirectly confirms the importance of vertical scheduling.

Finally, we compare the throughput of GreedySnake with the estimation from performance model. In most cases, the gap is quite small, caused by the unavoidable dynamic behavior such as pipeline bubble, and imbalanced operation time due to the resource contention that cannot be predicted accurately. We also observe that the gap can be slightly larger when the execution transitions from I/O-bound to compute-bound. This is because the pipeline around this period is more sensitive to the variability of the latency of individual operations. Additionally, we find that for GPT-65B with 4 GPUs, the gap is larger compared to others. This is because the cloud cluster is shared by multiple users, and as a result, the SSD bandwidth tends to diverge more from the performance model due to the sharing and contention of its bandwidth.

6.3 Benefits of Delayed Optimizer Step

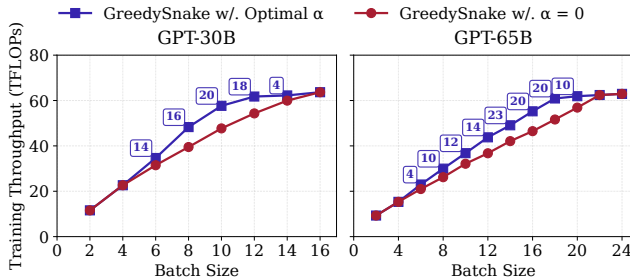


Figure 11: Training throughput w/. and w/o delaying optimizer step. Delaying factors α are annotated in percentage.

Figure 11 compares the throughput of GreedySnake with and without delayed optimizer step. For the latter, the delay ratio α is 0. We see that both cases eventually reach the same saturated throughput, but the delayed optimizer step reduces the batch size to reach that throughput. In other words, it

makes the I/O-bound phase closer to the ideal roofline, consistent with the fact that this mechanism mitigates the I/O bottleneck of optimizer step by extending its allowable execution period.

6.4 Benefits of Vertical Scheduling

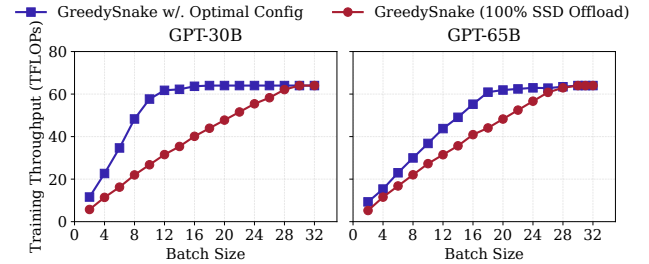


Figure 12: Training throughput achieved by 100% SSD-offloading vs optimal config.

In this section, we address a key question: is the throughput improvement driven by caching more training data in CPU memory, or by the *fundamental merits* of vertical scheduling? To answer this, we run an experiment under an extreme setting that forces all training data to be fully offloaded to SSD (i.e., CPU memory is used only for working buffers). As shown in Figure 12, compared to the earlier results using the best configuration found by our LP-based search, throughput increases more slowly. Crucially, even in this extreme setting, GreedySnake eventually reaches a *similar* saturated throughput. These results provide the strongest evidence that the intrinsic properties of vertical scheduling are the primary reason for the throughput improvement.

The *crux* of the advantage is that, when GreedySnake adds a new micro-batch to increase the global batch size, the additional computation time—the extra forward and backward work—is *greater than* the additional I/O time to move that micro-batch’s activation checkpoints. Consequently, each additional micro-batch yields *time “credit”* that can be used to overlap the optimizer step. For GPT-65B, for example, the forward and backward computation of one micro-batch takes 16.4 s, whereas the additional checkpoint I/O incurred by that micro-batch takes only 1.1 s. Because the former is much larger than the latter, GreedySnake can still reach—albeit more slowly—a similar saturated throughput even when no training data are allowed to remain in CPU memory: the time “credit” accumulates across micro-batches and eventually overlaps the entire optimizer step. From this perspective, we can unify the benefits of delaying the optimizer step and placing a fraction of training data in CPU memory: both are engineering techniques to *increase the time “credit”* contributed by each micro-batch, enabling the optimizer step to be overlapped with *fewer* micro-batches. However, they are not the determining factors for achieving a higher saturated throughput; *the vertical scheduling is*.

6.5 Training Accuracy

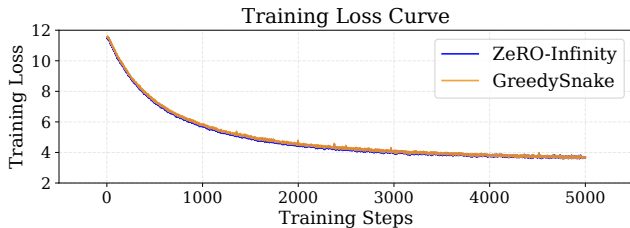


Figure 13: Training loss of GPT-30B on the Pile dataset.

Figure 13 compares the training loss curves of ZeRO-Infinity and GreedySnake. Both systems produce similar training loss despite minor discrepancies. After ruling out non-determinism from FlashAttention’s backward computation [9], we identify two causes. First, different scheduling methods lead to different dropout operation orders, which changes the loss. Second, in ZeRO-Infinity, when the optimizer computation size is not an exact multiple of the CPU’s SIMD width, the remaining elements are handled with scalar operations. In contrast, GreedySnake performs all computations with SIMD operations to ensure reproducible loss values across different partition ratios. These implementation differences account for the minor discrepancies observed.

7 Conclusion

This paper proposes GreedySnake, a novel SSD-offloaded training system that adopts *vertical scheduling*, where all micro-batches of a layer are executed before advancing to the next layer. To further alleviate the I/O bottleneck, GreedySnake overlaps part of the optimizer step with the forward pass of the next iteration. GreedySnake achieves higher throughput with smaller batch sizes. Experiments on NVIDIA A100 GPUs show that GreedySnake improves saturated training throughput over ZeRO-Infinity by $1.96\times$ (1 GPU) and $1.93\times$ (4 GPUs) for GPT-65B, and by $2.53\times$ (1 GPU) for GPT-175B.

References

- [1] OpenAI Sandhini Agarwal, Lama Ahmad, Jason Ai, Sam Altman, Andy Applebaum, Edwin Arbus, Rahul K. Arora, Yu Bai, Bowen Baker, Hai-Biao Bao, Boaz Barak, Ally Bennett, Tyler Bertao, Nivedita Brett, Eugene Brevdo, Greg Brockman, Sébastien Bubeck, Cheng Chang, Kai Chen, Mark Chen, Enoch Cheung, Aidan Clark, Dan Cook, Marat Dukhan, Casey Dvorak, K Fives, Vlad Fomenko, T. Garipov, Kristian Georgiev, Mia Glaese, Tarun Gogineni, A. B. Goucher, Lukas Gross, Katia Gil Guzman, John Hallman, Jackie Hehir, Johannes Heidecke, Alec Helyar, Haitang Hu, Romain Huet, Jacob Huh, Saachi Jain, Zach Johnson, Chris Koch, Irina Kofman, Dominika Kundel, Jason Kwon, Volodymyr Kyrylov, Elaine Ya Le, Guillaume Leclerc, James Lennon, Scott Lessans, Mario Lezcano-Casado, Yuanzhi Li, Zhuohan Li, Ji Lin, Jordan Liss, Lily Liu, Jiancheng Liu, Kevin Lu, Chris Lu, Zoran Martinovic, Lindsay McCallum, Josh McGrath, Scott McKinney, Aidan McLaughlin, Song Mei, Steve Mostovoy, Tong Mu, Gideon Myles, Alexander Neitz, Alex Nichol, Jakub W. Pachocki, Alex Paino, Dana Palmie, Ashley Pantuliano, Giambattista Parascandolo, Jongsoo Park, Leher Pathak, Carolina Paz, Ludovic Peran, Dmitry Pimenov, Michelle Pokrass, Elizabeth Proehl, Huida Qiu, Gaby Raila, Filippo Rasو, Hongyu Ren, Kimmy Richardson, David Robinson, Bob Rotsted, Hadi Salman, Suvansh Sanjeev, Max Schwarzer, Daniel Sculley, Harshit S. Sikchi, Kendal Simon, Karan Singhal, Yang Song, Dane Stuckey, Zhiqing Sun, Phil Tillet, Sam Toizer, Foivos Tsimpourlas, Nikhil Vyas, Eric Wallace, Xin Wang, Miles Wang, Olivia Watkins, Kevin Weil, Amy Wendling, Kevin Whinnery, Cedric Whitney, Hannah Wong, Lin Yang, Yu Yang, Michihiro Yasunaga, Kristen Ying, Wojciech Zaremba, Wenting Zhan, Cyril Zhang, Brian Zhang, Eddie Zhang, and Shengjia Zhao. gpt-oss-120b&gpt-oss-20b model card. 2025.
- [2] Jonghyun Bae, Jongsung Lee, Yunho Jin, Sam Son, Shine Kim, Hakbeom Jang, Tae Jun Ham, and Jae W Lee. Flashneuron: Ssd-enabled large-batch training of very deep neural networks. In *19th USENIX Conference on File and Storage Technologies (FAST 21)*, pages 387–401, 2021.
- [3] Jinze Bai, Shuai Bai, Yunfei Chu, Zeyu Cui, Kai Dang, Xiaodong Deng, Yang Fan, Wenhong Ge, Yu Han, Fei Huang, Binyuan Hui, Luo Ji, Mei Li, Junyang Lin, Runji Lin, Dayiheng Liu, Gao Liu, Chengqiang Lu, K. Lu, Jianxin Ma, Rui Men, Xingzhang Ren, Xuancheng Ren, Chuanqi Tan, Sinan Tan, Jianhong Tu, Peng Wang, Shijie Wang, Wei Wang, Shengguang Wu, Benfeng Xu, Jin Xu, An Yang, Hao Yang, Jian Yang, Jian Yang, Shusheng Yang, Yang Yao, Bowen Yu, Yu Bowen, Hongyi Yuan, Zheng Yuan, Jianwei Zhang, Xing Zhang, Yichang Zhang, Zhenru Zhang, Chang Zhou, Jingren Zhou, Xiaohuan Zhou, and Tianhang Zhu. Qwen technical report. *ArXiv*, abs/2309.16609, 2023.
- [4] Olivier Beaumont, Lionel Eyraud-Dubois, and Alena Shilova. Efficient combination of rematerialization and offloading for training dnns. *Advances in Neural Information Processing Systems*, 34:23844–23857, 2021.
- [5] Tom B. Brown, Benjamin Mann, Nick Ryder, Melanie Subbiah, Jared Kaplan, Prafulla Dhariwal, Arvind Neelakantan, Pranav Shyam, Girish Sastry, Amanda Askell, Sandhini Agarwal, Ariel Herbert-Voss, Gretchen Krueger, T. J. Henighan, Rewon Child, Aditya Ramesh,

- Daniel M. Ziegler, Jeff Wu, Clemens Winter, Christopher Hesse, Mark Chen, Eric Sigler, Mateusz Litwin, Scott Gray, Benjamin Chess, Jack Clark, Christopher Berner, Sam McCandlish, Alec Radford, Ilya Sutskever, and Dario Amodei. Language models are few-shot learners. *ArXiv*, abs/2005.14165, 2020.
- [6] Tianqi Chen, Bing Xu, Chiyuan Zhang, and Carlos Guestrin. Training deep nets with sublinear memory cost. *arXiv preprint arXiv:1604.06174*, 2016.
- [7] Aakanksha Chowdhery, Sharan Narang, Jacob Devlin, Maarten Bosma, Gaurav Mishra, Adam Roberts, Paul Barham, Hyung Won Chung, Charles Sutton, Sebastian Gehrmann, Parker Schuh, Kensen Shi, Sasha Tsvyashchenko, Joshua Maynez, Abhishek Rao, Parker Barnes, Yi Tay, Noam Shazeer, Vinodkumar Prabhakaran, Emily Reif, Nan Du, Ben Hutchinson, Reiner Pope, James Bradbury, Jacob Austin, Michael Isard, Guy Gur-Ari, Pengcheng Yin, Toju Duke, Anselm Levskaya, Sanjay Ghemawat, Sunipa Dev, Henryk Michalewski, Xavier García, Vedant Misra, Kevin Robinson, Liam Fedus, Denny Zhou, Daphne Ippolito, David Luan, Hyeontaek Lim, Barret Zoph, Alexander Spiridonov, Ryan Sepassi, David Dohan, Shivani Agrawal, Mark Omernick, Andrew M. Dai, Thanumalayan Sankaranarayana Pillai, Marie Pellat, Aitor Lewkowycz, Erica Moreira, Rewon Child, Oleksandr Polozov, Katherine Lee, Zongwei Zhou, Xuezhi Wang, Brennan Saeta, Mark Díaz, Orhan Firat, Michele Catasta, Jason Wei, Kathleen S. Meier-Hellstern, Douglas Eck, Jeff Dean, Slav Petrov, and Noah Fiedel. Palm: Scaling language modeling with pathways. *ArXiv*, abs/2204.02311, 2022.
- [8] Vasek Chvátal. *Linear Programming*. W.H. Freeman, New York, 1983.
- [9] Tri Dao. Flashattention-2: Faster attention with better parallelism and work partitioning. In *The Twelfth International Conference on Learning Representations*, 2024.
- [10] DeepSeek-AI, Aixin Liu, Bei Feng, Bing Xue, Bingxuan Wang, Bochao Wu, Chengda Lu, Chenggang Zhao, Chengqi Deng, Chenyu Zhang, Chong Ruan, Damai Dai, Daya Guo, Dejian Yang, Deli Chen, Dongjie Ji, Erhang Li, Fangyun Lin, Fucong Dai, Fuli Luo, Guangbo Hao, Guanting Chen, Guowei Li, H. Zhang, Han Bao, Hanwei Xu, Haocheng Wang, Haowei Zhang, Honghui Ding, Huajian Xin, Huazuo Gao, Hui Li, Hui Qu, J. L. Cai, Jian Liang, Jianzhong Guo, Jiaqi Ni, Jiashi Li, Jiawei Wang, Jin Chen, Jingchang Chen, Jingyang Yuan, Junjie Qiu, Junlong Li, Junxiao Song, Kai Dong, Kai Hu, Kaige Gao, Kang Guan, Kexin Huang, Kuai Yu, Lean Wang, Lecong Zhang, Lei Xu, Leyi Xia, Liang Zhao, Litong Wang, Liyue Zhang, Meng Li, Miaojun Wang, Mingchuan Zhang, Minghua Zhang, Minghui Tang, Mingming Li, Ning Tian, Panpan Huang, Peiyi Wang, Peng Zhang, Qiancheng Wang, Qihao Zhu, Qinyu Chen, Qiushi Du, R. J. Chen, R. L. Jin, Ruiqi Ge, Ruisong Zhang, Ruizhe Pan, Runji Wang, Runxin Xu, Ruoyu Zhang, Ruyi Chen, S. S. Li, Shanghao Lu, Shangyan Zhou, Shanhuang Chen, Shaoqing Wu, Shengfeng Ye, Shengfeng Ye, Shirong Ma, Shiyu Wang, Shuang Zhou, Shuiping Yu, Shunfeng Zhou, Shuting Pan, T. Wang, Tao Yun, Tian Pei, Tianyu Sun, W. L. Xiao, Wangding Zeng, Wanjia Zhao, Wei An, Wen Liu, Wenfeng Liang, Wenjun Gao, Wenzheng Yu, Wentao Zhang, X. Q. Li, Xiangyue Jin, Xianzu Wang, Xiao Bi, Xiaodong Liu, Xiaohan Wang, Xiaojin Shen, Xiaokang Chen, Xiaokang Zhang, Xiaosha Chen, Xiaotao Nie, Xiaowen Sun, Xiaoxiang Wang, Xin Cheng, Xin Liu, Xin Xie, Xingchao Liu, Xingkai Yu, Xinnan Song, Xinxia Shan, Xinyi Zhou, Xinyu Yang, Xinyuan Li, Xuecheng Su, Xuheng Lin, Y. K. Li, Y. Q. Wang, Y. X. Wei, Y. X. Zhu, Yang Zhang, Yanhong Xu, Yanhong Xu, Yanping Huang, Yao Li, Yao Zhao, Yaofeng Sun, Yaohui Li, Yaohui Wang, Yi Yu, Yi Zheng, Yichao Zhang, Yifan Shi, Yiliang Xiong, Ying He, Ying Tang, Yishi Piao, Yisong Wang, Yixuan Tan, Yiyang Ma, Yiyuan Liu, Yongqiang Guo, Yu Wu, Yuan Ou, Yuchen Zhu, Yuduan Wang, Yue Gong, Yuheng Zou, Yujia He, Yukun Zha, Yunfan Xiong, Yunxian Ma, Yuting Yan, Yuxiang Luo, Yuxiang You, Yuxuan Liu, Yuyang Zhou, Z. F. Wu, Z. Z. Ren, Zehui Ren, Zhangli Sha, Zhe Fu, Zhean Xu, Zhen Huang, Zhen Zhang, Zhenda Xie, Zhengyan Zhang, Zhewen Hao, Zhibin Gou, Zhicheng Ma, Zhigang Yan, Zhihong Shao, Zhipeng Xu, Zhiyu Wu, Zhongyu Zhang, Zhuoshu Li, Zihui Gu, Zijia Zhu, Zijun Liu, Zilin Li, Ziwei Xie, Ziyang Song, Ziyi Gao, and Zizheng Pan. Deepseek-v3 technical report, 2025.
- [11] Jiarui Fang, Zilin Zhu, Shenggui Li, Hui Su, Yang Yu, Jie Zhou, and Yang You. Parallel training of pre-trained models via chunk-based dynamic memory management. *IEEE Transactions on Parallel and Distributed Systems*, 34(1):304–315, 2022.
- [12] Mark Hildebrand, Jawad Khan, Sanjeev Trika, Jason Lowe-Power, and Venkatesh Akella. Autotm: Automatic tensor movement in heterogeneous memory systems using integer linear programming. In *Proceedings of the Twenty-Fifth International Conference on Architectural Support for Programming Languages and Operating Systems*, pages 875–890, 2020.
- [13] Chien-Chin Huang, Gu Jin, and Jinyang Li. Swapadvisor: Pushing deep learning beyond the gpu memory limit via smart swapping. In *Proceedings of the Twenty-Fifth International Conference on Architectural Support for Programming Languages and Operating Systems*, pages 1341–1355, 2020.

- [14] Paras Jain, Ajay Jain, Aniruddha Nrusimha, Amir Gholami, Pieter Abbeel, Joseph Gonzalez, Kurt Keutzer, and Ion Stoica. Checkmate: Breaking the memory wall with optimal tensor rematerialization. *Proceedings of Machine Learning and Systems*, 2:497–511, 2020.
- [15] Hongsun Jang, Jaeyong Song, Jaewon Jung, Jaeyoung Park, Youngsok Kim, and Jinho Lee. Smart-infinity: Fast large language model training using near-storage processing on a real system. In *2024 IEEE International Symposium on High-Performance Computer Architecture (HPCA)*, pages 345–360. IEEE, 2024.
- [16] Jared Kaplan, Sam McCandlish, T. J. Henighan, Tom B. Brown, Benjamin Chess, Rewon Child, Scott Gray, Alec Radford, Jeff Wu, and Dario Amodei. Scaling laws for neural language models. *ArXiv*, abs/2001.08361, 2020.
- [17] Diederik P. Kingma and Jimmy Ba. Adam: A method for stochastic optimization, 2017.
- [18] Xinyu Lian, Masahiro Tanaka, Olatunji Ruwase, and Minjia Zhang. Superoffload: Unleashing the power of large-scale llm training on superchips. *arXiv preprint arXiv:2509.21271*, 2025.
- [19] Wanchao Liang, Tianyu Liu, Less Wright, Will Constable, Andrew Gu, Chien-Chin Huang, Iris Zhang, Wei Feng, Howard Huang, Junjie Wang, et al. Torch titan: One-stop pytorch native solution for production ready llm pre-training. *arXiv preprint arXiv:2410.06511*, 2024.
- [20] Changyue Liao, Mo Sun, Zihan Yang, Jun Xie, Kaiqi Chen, Binhang Yuan, Fei Wu, and Zeke Wang. Ratel: Optimizing holistic data movement to fine-tune 100b model on a consumer gpu. In *2025 IEEE 41st International Conference on Data Engineering (ICDE)*, pages 292–306, 2025.
- [21] Paulius Micikevicius, Sharan Narang, Jonah Alben, Gregory Diamos, Erich Elsen, David Garcia, Boris Ginsburg, Michael Houston, Oleksii Kuchaiev, Ganesh Venkatesh, and Hao Wu. Mixed precision training. In *International Conference on Learning Representations*, 2018.
- [22] Adam Paszke, Sam Gross, Francisco Massa, Adam Lerer, James Bradbury, Gregory Chanan, Trevor Killeen, Zeming Lin, Natalia Gimelshein, Luca Antiga, Alban Desmaison, Andreas Kopf, Edward Yang, Zachary DeVito, Martin Raison, Alykhan Tejani, Sasank Chilamkurthy, Benoit Steiner, Lu Fang, Junjie Bai, and Soumith Chintala. Pytorch: An imperative style, high-performance deep learning library. In *Advances in Neural Information Processing Systems 32*, pages 8024–8035. Curran Associates, Inc., 2019.
- [23] Xuan Peng, Xuanhua Shi, Hulin Dai, Hai Jin, Weiliang Ma, Qian Xiong, Fan Yang, and Xuehai Qian. Cappuchin: Tensor-based gpu memory management for deep learning. In *Proceedings of the Twenty-Fifth International Conference on Architectural Support for Programming Languages and Operating Systems*, pages 891–905, 2020.
- [24] Samyam Rajbhandari, Jeff Rasley, Olatunji Ruwase, and Yuxiong He. Zero: Memory optimizations toward training trillion parameter models. In *SC20: International Conference for High Performance Computing, Networking, Storage and Analysis*, pages 1–16. IEEE, 2020.
- [25] Samyam Rajbhandari, Olatunji Ruwase, Jeff Rasley, Shaden Smith, and Yuxiong He. Zero-infinity: breaking the gpu memory wall for extreme scale deep learning. In *Proceedings of the International Conference for High Performance Computing, Networking, Storage and Analysis, SC ’21*, New York, NY, USA, 2021. Association for Computing Machinery.
- [26] Jie Ren, Jiaolin Luo, Kai Wu, Minjia Zhang, Hyeran Jeon, and Dong Li. Sentinel: Efficient tensor migration and allocation on heterogeneous memory systems for deep learning. In *2021 IEEE International Symposium on High-Performance Computer Architecture (HPCA)*, pages 598–611. IEEE, 2021.
- [27] Jie Ren, Samyam Rajbhandari, Reza Yazdani Am-inabadi, Olatunji Ruwase, Shuangyan Yang, Minjia Zhang, Dong Li, and Yuxiong He. Zero-offload: Democratizing billion-scale model training. In *2021 USENIX Annual Technical Conference (USENIX ATC 21)*, pages 551–564, 2021.
- [28] Minsoo Rhu, Natalia Gimelshein, Jason Clemons, Arslan Zulfiqar, and Stephen W Keckler. vdnn: Virtualized deep neural networks for scalable, memory-efficient neural network design. In *2016 49th Annual IEEE/ACM International Symposium on Microarchitecture (MICRO)*, pages 1–13. IEEE, 2016.
- [29] Mohammad Shoeybi, Mostofa Patwary, Raul Puri, Patrick LeGresley, Jared Casper, and Bryan Catanzaro. Megatron-lm: Training multi-billion parameter language models using model parallelism. *arXiv preprint arXiv:1909.08053*, 2019.
- [30] Xiaoyang Sun, Wei Wang, Shenghao Qiu, Renyu Yang, Songfang Huang, Jie Xu, and Zheng Wang. Stronghold: fast and affordable billion-scale deep learning model training. In *Proceedings of the International Conference on High Performance Computing, Networking, Storage and Analysis, SC ’22*. IEEE Press, 2022.

- [31] Ashish Vaswani, Noam Shazeer, Niki Parmar, Jakob Uszkoreit, Llion Jones, Aidan N Gomez, Łukasz Kaiser, and Illia Polosukhin. Attention is all you need. *Advances in neural information processing systems*, 30, 2017.
- [32] Linnan Wang, Jinmian Ye, Yiyang Zhao, Wei Wu, Ang Li, Shuaiwen Leon Song, Zenglin Xu, and Tim Kraska. Superneurons: Dynamic gpu memory management for training deep neural networks. In *Proceedings of the 23rd ACM SIGPLAN symposium on principles and practice of parallel programming*, pages 41–53, 2018.
- [33] Kun Wu, Jeongmin Brian Park, Xiaofan Zhang, Mert Hidayetoğlu, Vikram Sharma Mailthody, Sitalo Huang, Steven Sam Lumetta, and Wen mei Hwu. Ssdtrain: An activation offloading framework to ssds for faster large language model training, 2025.
- [34] Tailing Yuan, Yuliang Liu, Xucheng Ye, Shenglong Zhang, Jianchao Tan, Bin Chen, Chengru Song, and Di Zhang. Accelerating the training of large language models using efficient activation rematerialization and optimal hybrid parallelism. In *2024 USENIX Annual Technical Conference (USENIX ATC 24)*, pages 545–561, 2024.
- [35] Ziqi Yuan, Haoyang Zhang, Yirui Eric Zhou, Apoorve Mohan, I Chung, Seetharami Seelam, Jian Huang, et al. Cost-efficient llm training with lifetime-aware tensor offloading via gpudirect storage. *arXiv preprint arXiv:2506.06472*, 2025.
- [36] Yanli Zhao, Andrew Gu, Rohan Varma, Liang Luo, Chien-Chin Huang, Min Xu, Less Wright, Hamid Shojanazeri, Myle Ott, Sam Shleifer, et al. Pytorch fsdp: experiences on scaling fully sharded data parallel. *arXiv preprint arXiv:2304.11277*, 2023.